Electronic Supplementary Information

In situ synthesis of pyridinium-based ionic porous organic polymers with hydroxide anions and pyridinyl radicals for halogen-free catalytic fixation of atmospheric CO_2

Ke Liu, Zixuan Xu, He Huang, Yadong Zhang, Yan Liu, Zhiheng Qiu, Minman Tong, Zhouyang Long and Guojian Chen*

School of Chemistry and Materials Science, Jiangsu Key Laboratory of Green Synthetic Chemistry for Functional Materials, Jiangsu Normal University, Xuzhou, 221116, China.

*Corresponding author, E-mail: gjchen@jsnu.edu.cn

Experimental Section

Materials

3-Pyridineacetonitrile, benzene-1,3,5-tricarbaldehyde, α,α'-dibromo-*p*-xylene, KOH, NaOH, Cs_2CO_3, the epoxide substrates, common solvents and reagents were commercially available and used without further purification.

Methods

Liquid-state ^{1}H and ^{13}C NMR spectra were measured with a Bruker DPX 500 spectrometer at ambient temperature. Solid-state ^{13}C cross-polarization/magic angle spinning (CP/MAS) NMR spectra were carried out on a Bruker AVANCE III 600 spectrometer. The CHN elemental analysis was performed on an elemental analyzer Vario EL cube. Chemical compositions and states of the samples were determined by the X-ray photoelectron spectroscopy (XPS, Thermo ESCALAB 250Xi). Electron paramagnetic resonance (EPR) spectra were recorded on a Bruker EMX-10/12 spectrometer at the X-band at room temperature. Fourier transform infrared spectroscopy (FTIR) was recorded on a Bruker Vertex 80V FT-IR instrument (KBr discs) in the region 4000-400 cm^{-1}. Thermogravimetric analysis (TGA) was carried out with a TA Q50 instrument in nitrogen atmosphere at a heating rate of 10 ^{o}C min^{-1}, while the sample was dried in vacuum at 100 ^{o}C for 12 h before analysis. X-ray diffraction (XRD) patterns were collected on the Bruker D8 Advance powder diffractometer using Ni-filtered Cu Ka radiation source at 40 kV and 20 mA, from 5 to 80^{o} with a scan rate of 0.2^{o} s^{-1}. Field emission scanning electron microscope (FESEM, Hitachi SU8010) was used to study the morphology. N_2 adsorption-desorption isotherms were measured at 77 K using a Quantachrome autosorb iQ2 analyzer, and the surface area of samples was calculated using the Brunauer-Emmett-Teller (BET) method and the pore size distribution was determined by the Barrett-Joyner-Halenda (BJH) model, while the samples were degassed at 150 °C for 10 h in high vacuum before analysis.

Synthesis of the acetonitrile-functionalized pyridinium-based ionic liquid (IL-ACN)

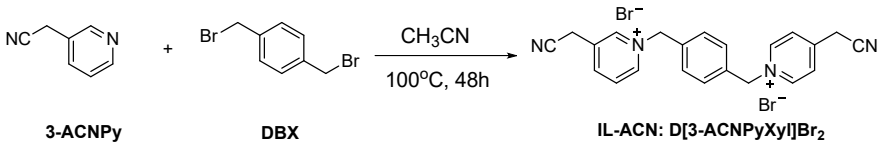

Scheme S1 Synthesis of the acetonitrile-functionalized pyridinium-based IL-ACN.

The targeted acetonitrile-functionalized pyridinium-based ionic liquid was prepared by the quaternization reaction of 3-pyridineacetonitrile (3-ACNPy) and α,α'-dibromo-*p*-xylene (DBX) as follows (Scheme S1). First, the

raw materials 3-ACNPy (4 mmol, 0.4726 g) and DBX (2 mmol, 0.5279 g) were dissolved in the solvent of CH_3CN (40 mL), and then the mixture were added into a 50 mL Teflon-lined autoclave with stirred for 20 minutes at room temperature. Subsequently, the reaction was taken place at 100 °C in a constant temperature oven for 48 h. After reaction, the obtained white solid was dispersed into ethyl acetate (20 mL) with stirring for 0.5 h. At last, the above suspension was filtrated, washed with ethyl acetate for several times, and dried at 80 °C for 12 h in vacuum to give a white powder solid (IL-ACN: D[3-ACNPyXyl]Br_2) with a high yield of 91%.

D[3-ACNPyXyl]Br_2: ^{1}H NMR (400 MHz, D_2O) (Fig. S1A): δ=8.94~8.98 (C*H*, 4H), 8.61~8.63 (C*H*, 2H), 8.11~8.14 (C*H*, 2H), 7.56~7.57 (CH_2, 4H), 5.90 (CH_2, 4H) and 4.25~4.26 ppm (CH_2, 4H). ^{13}C NMR (100 MHz, D_2O) (Fig. S1B): δ=145.93, 144.06, 143.67, 134.11, 133.18, 130.11, 128.58, 116.94, 64.14 and 20.78 ppm. Elemental analysis found: C, 52.53; H, 4.15; N, 11.42 wt%. Theoretical calcd. value for $C_{22}H_{20}N_4Br_2$ (MW: 500.23): C, 52.82; H, 4.03; N, 11.20 wt%.

Synthesis of pyridinium-based ionic porous organic polymers

Pyridinium-based ionic porous organic polymers (Py-iPOPs) were prepared by the Knoevenagel condensation reaction between the monomers benzene-1,3,5-tricarbaldehyde (TFB) and IL-ACN under basic conditions, as depicted in Scheme 1. In detail, TFB (0.2 mmol, 0.0324 g) was dissolved in the solvent of DMF (5 mL), IL-ACN (0.3 mmol, 0.1501 g) was dissolved in the solvent of DMF (5 mL) and H_2O (1.5 mL), and then the above two solutions were mixed together. At the same time, the base catalyst KOH (0.6 mmol, 0.034 g) that dissolved in 0.5 mL of water was added into the mixture solution. Subsequently, the above homogeneous mixture solution was moved into a 25 mL Teflon-lined autoclave. The static reaction was taken place in a constant temperature oven at 120 °C for 72 h. After reaction, the resulting precipitates was dispersed into H_2O (50 mL) with vigorous stirring for 12 h, the above suspension was filtered and washed with water, tetrahydrofuran (THF) and ethanol in sequence for several times to obtain a brown solid. At last, the solid was dried under vacuum at 80 °C for 12 h to give a yellowish-brown powder (Py-iPOP-1) with a desired solid yield of 54%. Elemental analysis found for Py-iPOP-1: C, 67.97; H, 5.16; N, 11.25 wt%. Theoretical calcd. value for Py-iPOP-1 based on the stoichiometric structure (*n*(TFB):*n*(IL-ACN)=2:3) with OH^- anions and some absorbed H_2O molecules $(C_{84}H_{60}N_{12}\bullet 3OH^-\bullet 11H_2O)_n$: C, 67.86; H, 5.76; N, 11.31 wt%.

To replace KOH with different base catalysts including NaOH and Cs_2CO_3, two control polymers named Py-iPOP-2 (solid yield 51%) and Py-iPOP-3 (solid yield 56%) were also prepared using similar reaction processes (Scheme S2 and S3). For Py-iPOP-2: elemental analysis found: C, 67.81; H, 5.04; N, 11.01 wt%. Theoretical calcd.

value for Py-iPOP-2 based on the stoichiometric structure with OH^- anions and some absorbed H_2O molecules $(C_{84}H_{60}N_{12}•3OH^-•11H_2O)_n$: C, 67.86; H, 5.76; N, 11.31 wt%. For Py-iPOP-3, elemental analysis found: C, 66.66; H, 5.18; N, 10.99 wt%. Theoretical calcd. value for Py-iPOP-3 based on the stoichiometric structure with CO_3^{2-} anions and some absorbed H_2O molecules $(C_{84}H_{60}N_{12}•1.5CO_3^{2-}•11H_2O)_n$: C, 67.31; H, 5.42; N, 11.02 wt%. By comparison, the experimental elemental analysis values of Py-iPOPs are well accord with their theoretical values, indicating that the rational synthesis of the targeted polymers.

Catalytic tests

The catalytic CO_2 cycloaddition reactions with epoxides into cyclic carbonates were carried out in a 25 mL Schlenk tube with a magnetic stirrer. As a typical run, epoxide (2 mmol) and the catalyst Py-iPOP-1 (40 mg) were added into placed in a Schlenk tube connected with a CO_2 balloon (0.1 MPa). And then, the mixture was stirred at the targeted temperature for a desired time. After the reaction, 3 mL of ethyl acetate was added into the reaction system, and then, the mixture was stirred for 0.5 h. Subsequently, the solid catalyst was separated by centrifugation, and the crude products were obtained by concentrating under reduced pressure and then were directly analyzed by the ^1H NMR spectroscopy to determine the yields of cyclic carbonates. For the catalyst recycling experiments, the reaction was performed under the same reaction conditions each time using the recovered catalyst. The reusability of the catalyst was tested in five-run cycling experiments. The solid catalyst was collected by centrifuged, washed with ethanol, dried in vacuum and used to the next run.

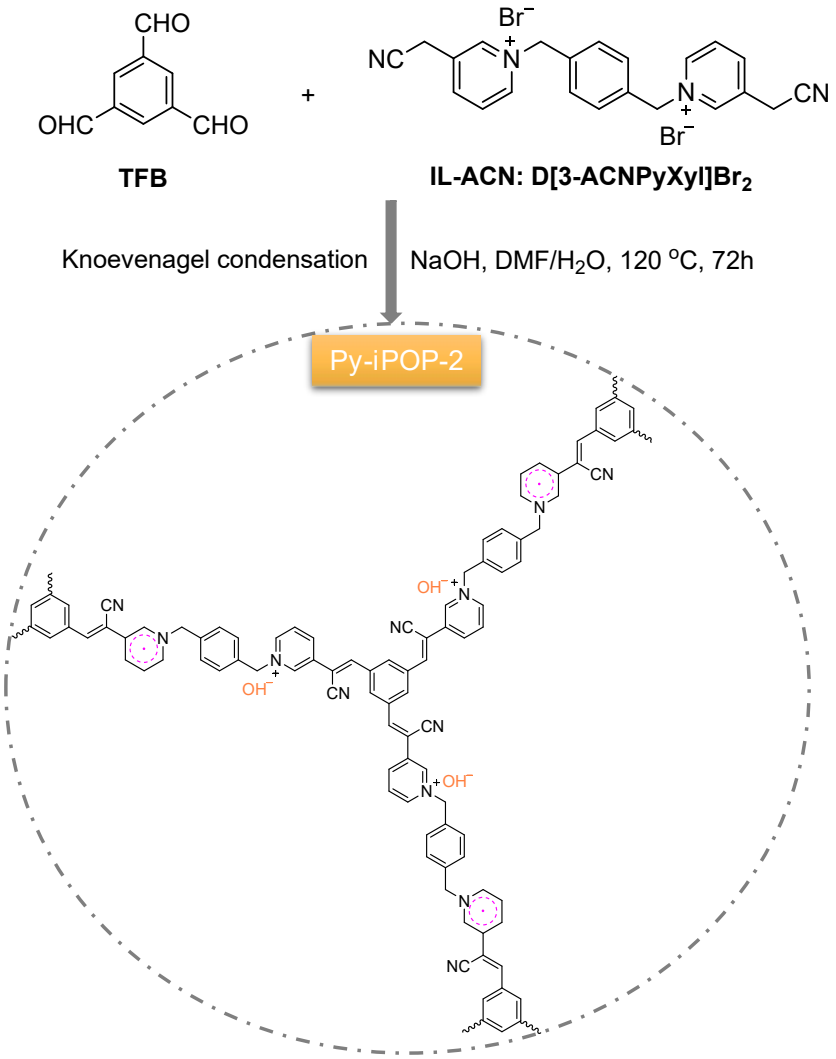

Scheme S2 Synthesis of the pyridinium-based ionic porous organic polymer (Py-iPOP-2) by the NaOH-catalyzed Knoevenagel condensation reaction. Note: the orange background for Py-iPOP-2 represents the difference in elemental compositions from Py-iPOP-1 with similar chemical structures.

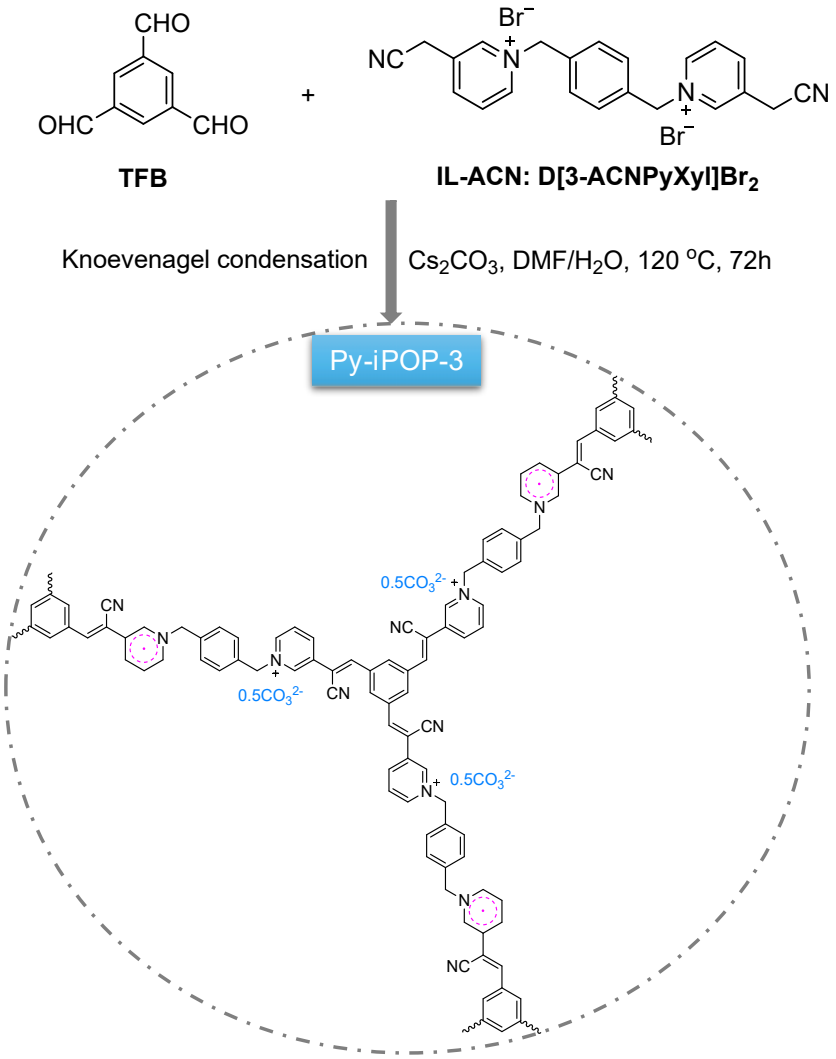

Scheme S3 Synthesis of the pyridinium-based ionic porous organic polymer (Py-iPOP-3) by the Cs_2CO_3-catalyzed Knoevenagel condensation reaction.

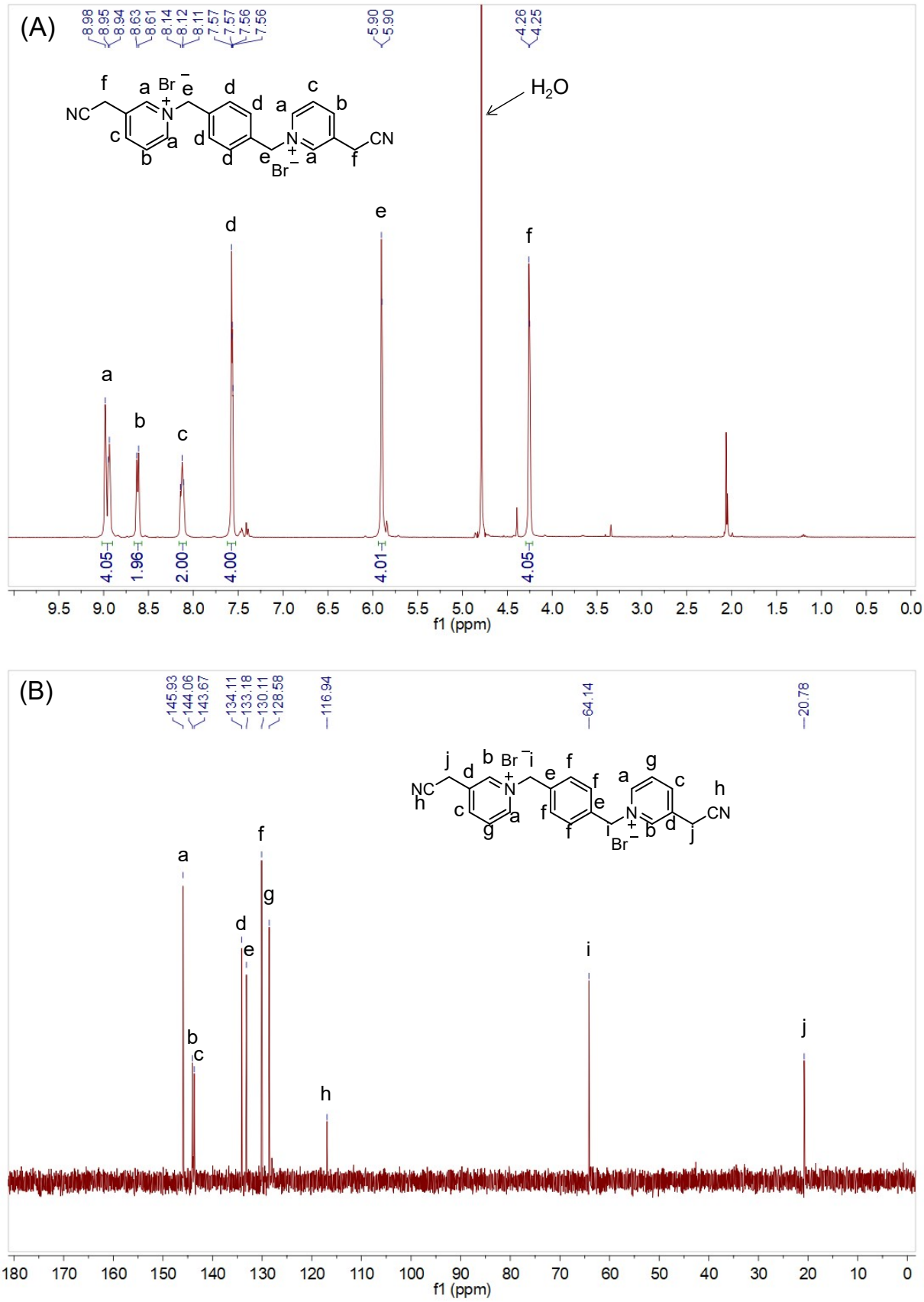

Fig. S1 (A) ^{1}H NMR and (B) ^{13}C NMR of D[3-ACNPyXyl]Br_2 using D_2O as the solvent.

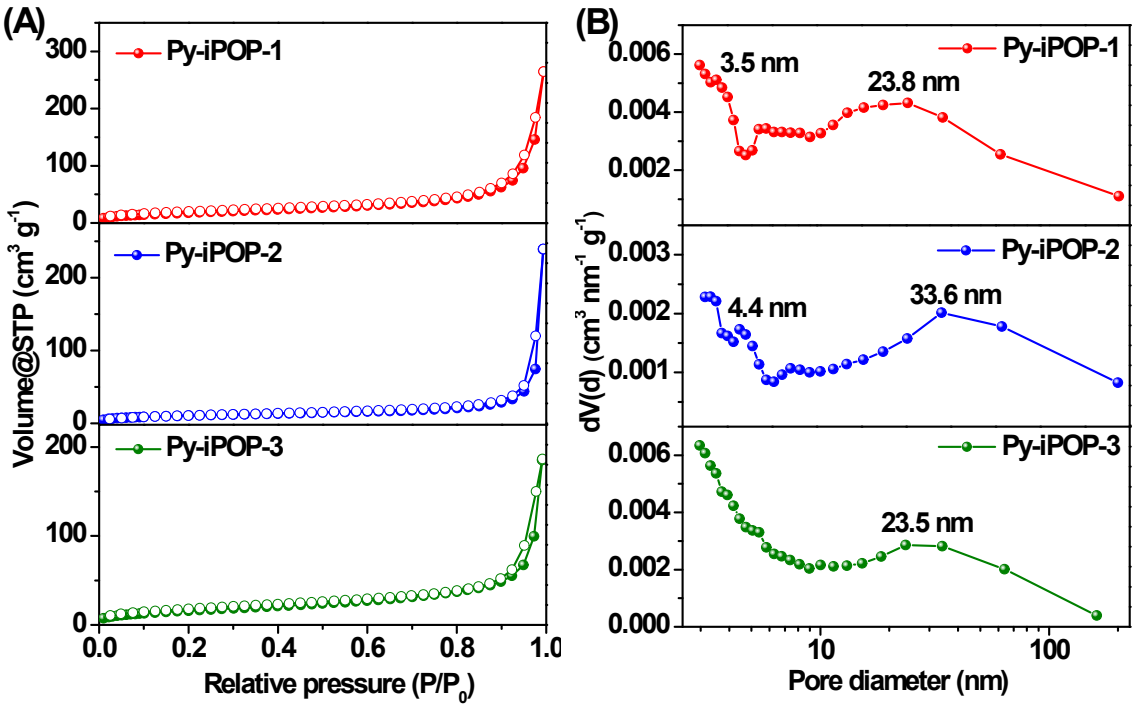

Fig. S2 (A) N_2 adsorption-desorption isotherms and (B) pore size distributions of Py-iPOP-1, Py-iPOP-2 and Py-iPOP-3 calculated by the BJH method.

Table S1 Synthetic parameters and porous textural properties of Py-iPOPs using different base catalysts.[a]

Samples	Base	Polymer Yield (%)	N content (wt%) [b]	Py-IL content (mmol g^{-1}) [c]	S_{BET} (m^2 g^{-1}) [d]	V_{total} (cm^3 g^{-1}) [e]	D_p (nm) [f]
Py-iPOP-1	KOH	54%	11.25	2.01	65	0.41	25.0
Py-iPOP-2	NaOH	51%	11.01	1.97	39	0.37	38.6
Py-iPOP-3	Cs_2CO_3	56%	10.99	1.96	60	0.29	19.5

[a] Reaction conditions: TFB (0.2 mmol), IL-ACN (0.3 mmol), base catalysts (0.6 mmol), DMF (10 mL), H_2O (1.5 mL), 120 °C, 72 h. [b] The N content (wt%) was obtained by the CHN elemental analysis. [c] The Py-IL content (mmol g^{-1})=0.25×1000×N content (wt%)/14. [d] BET surface areas were calculated over the range P/P_0=0.05~0.20. [e] Total pore volumes were calculated at P/P_0=0.99. [f] Average pore sizes.

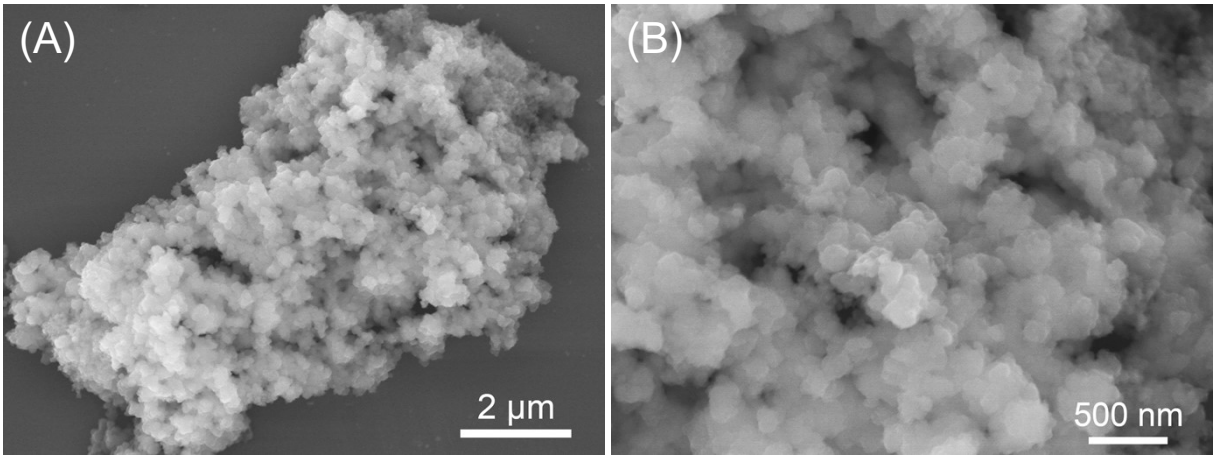

Fig. S3 SEM images of Py-iPOP-1.

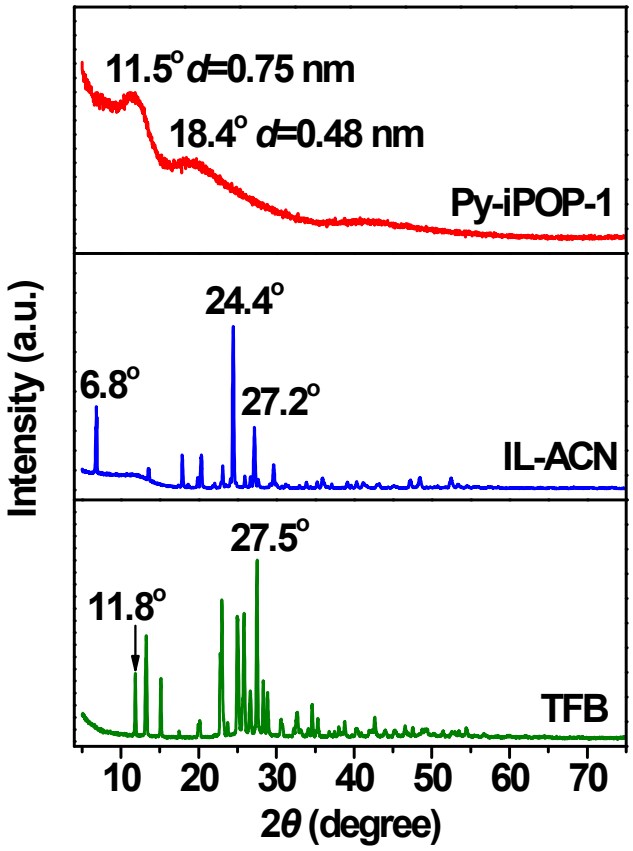

Fig. S4 X-ray diffraction patterns (XRD) patterns of TFB, IL-ACN and Py-iPOP-1.

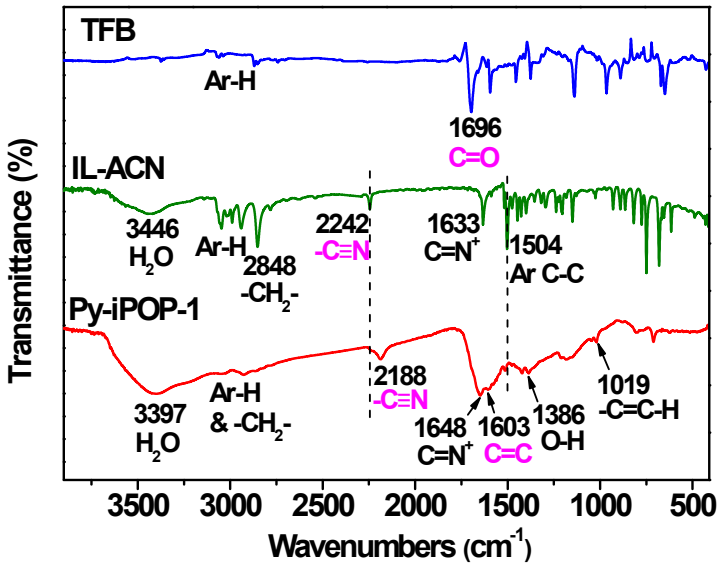

Fig. S5 FTIR spectra of TFB, IL-ACN and Py-iPOP-1.

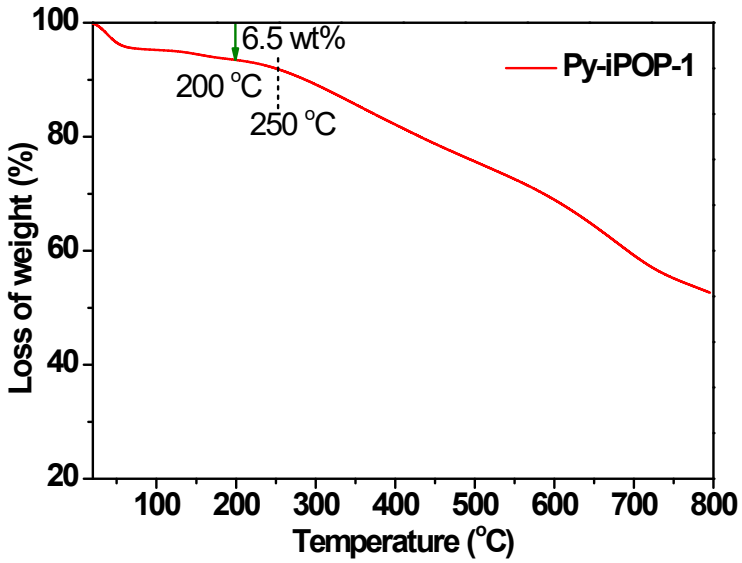

Fig. S6 The thermogravimetric analysis (TGA) curve of Py-iPOP-1 under N_2 atmosphere.

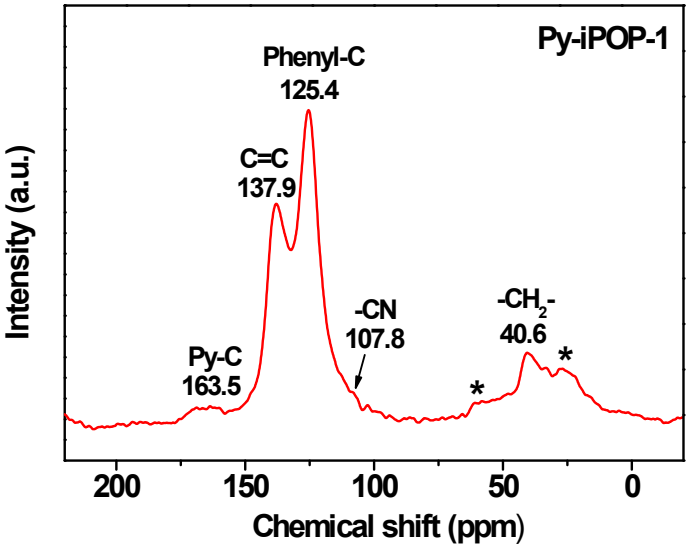

Fig. S7 The solid-state ^{13}C CP/MAS NMR spectrum of Py-iPOP-1.

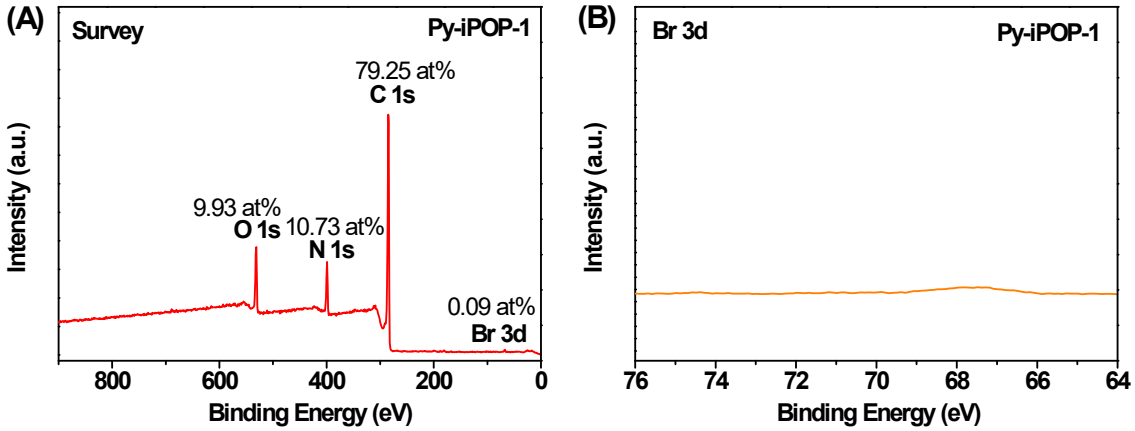

Fig. S8 XPS spectra of Py-iPOP-1: (A) Survey: atomic concentrations for C, N, O and Br, and (B) Br 3d.

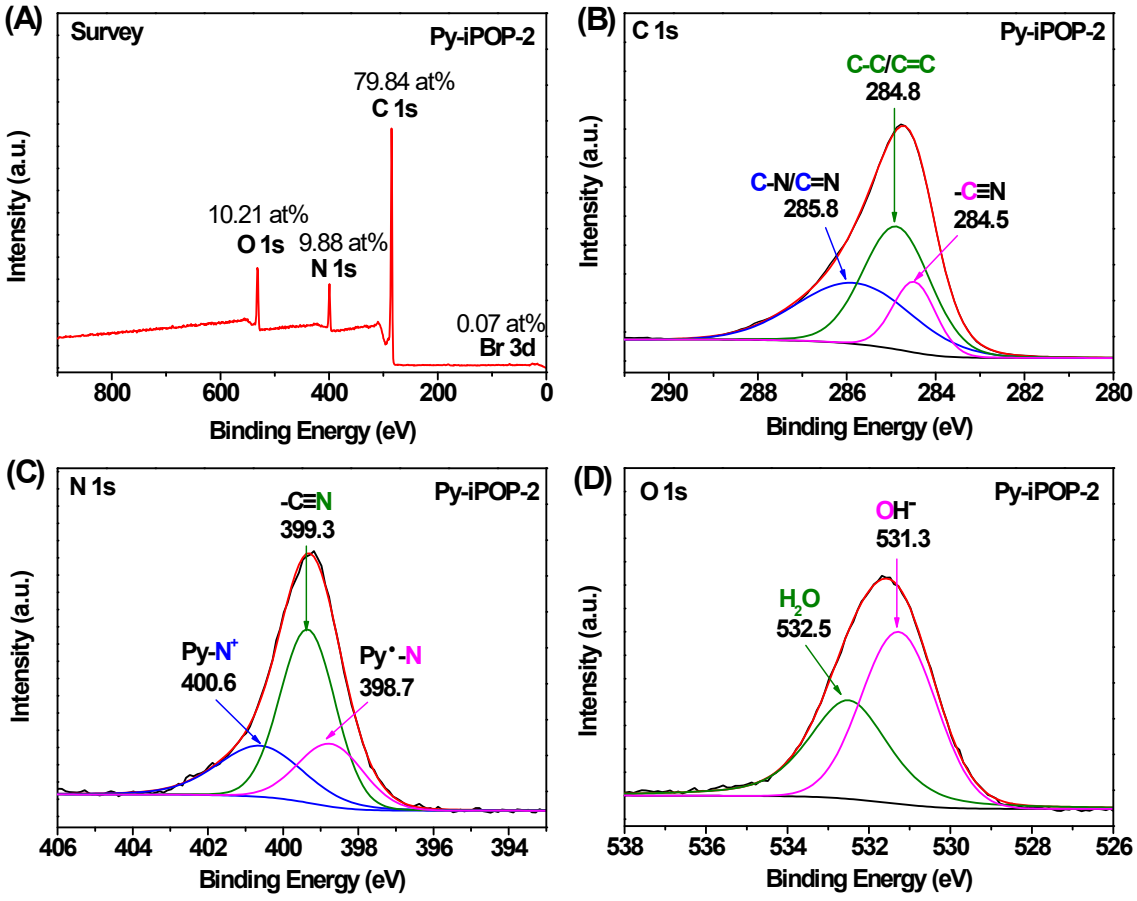

Fig. S9 XPS spectra of Py-iPOP-2: (A) Survey, (B) C 1s, (C) N 1s and (D) O 1s.

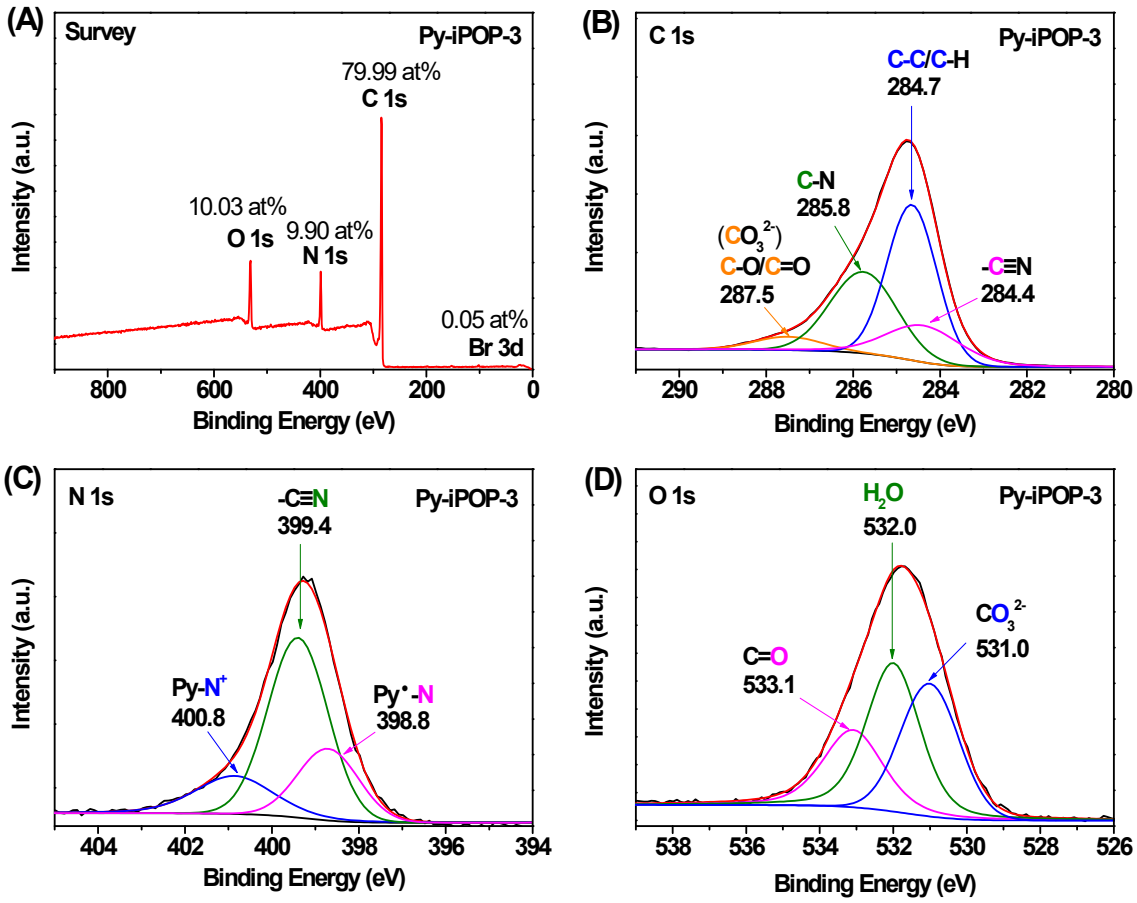

Fig. S10 XPS spectra of Py-iPOP-3: (A) Survey, (B) C 1s, (C) N 1s and (D) O 1s.

Table S2 Comparisons of the catalytic performances of different metal-free and halogen-free organic polymer heterogeneous catalysts for the cycloaddition reaction of CO_2 with epichlorohydrin (ECH).

Entry	Catalysts	Reaction conditions	Yield (%) [c]	Ref.
1	CUP	ECH (10 g), Cat. (10 wt%), CO_2 (6 MPa), 120 °C, 12 h	99	S1
2	MOP-0	ECH (10 mmol), Cat. (50 mg), CO_2 (1 MPa), 100 °C, 24 h	89	S2
3	PNHC	ECH (18 mmol), Cat. (104 mg), CO_2 (6.9 bar), 130 °C, 4 h	94.3	S3
4	2,5-DCP-CTF-0	ECH (18 mmol), Cat. (100 mg), CO_2 (6.9 bar), 130 °C, 4 h	95	S4
5	NP-NHC	ECH (5 mmol), Cat. (5 wt%), CO_2 (0.1 MPa), 120 °C, 24 h	98	S5
6	pyridyl salicylimine catalyst 1	ECH (5 mmol), Cat. (30 mg), CO_2 (0.1 MPa), 100 °C, 24 h	98	S6
7	PAD-3	ECH (5 mmol), Cat. (100 mg), CO_2 (0.1 MPa), 70 °C, 24 h	98	S7
8	[PAD][IDA]	ECH (5 mmol), Cat. (50 mg), CO_2 (0.1 MPa), 65 °C, 24 h	94	S8
9	PEAMC1	ECH (10 mmol), Cat. (100 mg), CO_2 (0.1 MPa), 70 °C, 48 h	95.3	S9
10	**Py-iPOP-1**	**ECH (2 mmol), Cat. (40 mg), CO_2 (0.1 MPa), 60 °C, 48 h**	**99**	**This work**

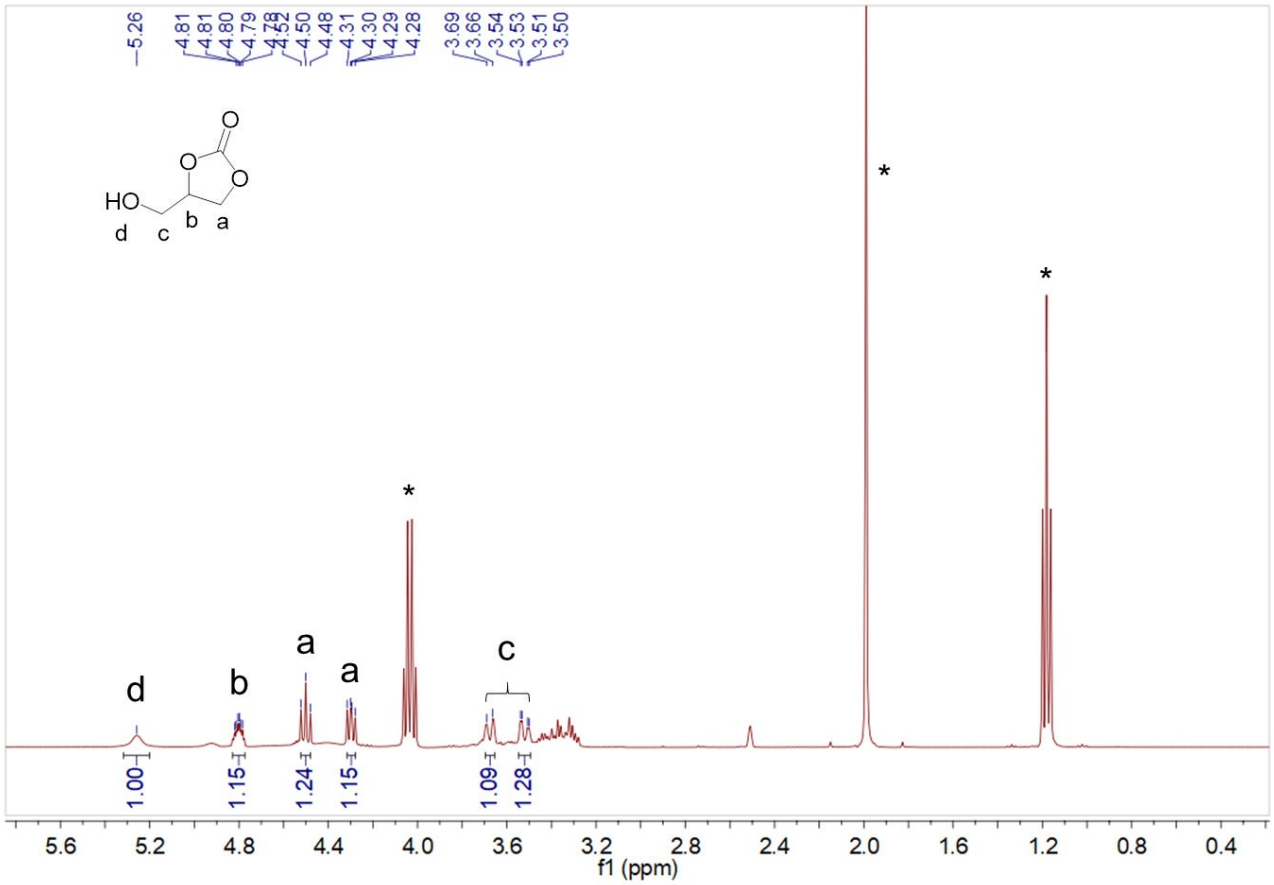

Fig. S11 ^{1}H NMR spectrum of 4-(hydroxymethyl)-1,3-dioxolan-2-one (400 MHz, d_6-DMSO): δ=5.26 (1H, OH), 4.81~4.78 (1H, OCH), 4.52~4.48 (1H, CH_2O), 4.31~4.28 (1H, CH_2O), 3.69~3.66 (1H, CH_2OH), and 3.54~3.50 ppm (1H, CH_2OH). * represents the residual solvent ethyl acetate. Reaction conditions: 60 ^{o}C, 48 h, yield of 99%.

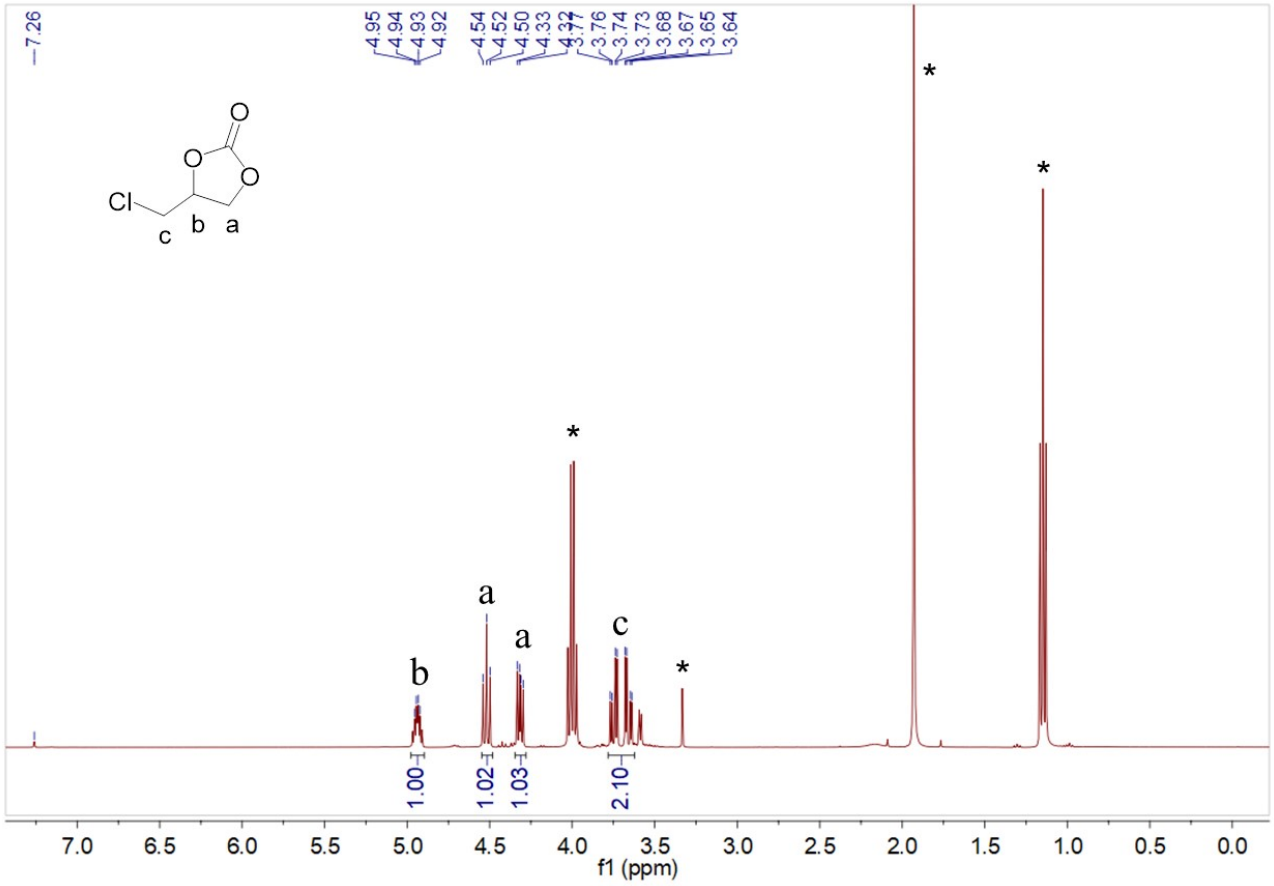

Fig. S12 ^{1}H NMR spectrum of 4-(chloromethyl)-1,3-dioxolan-2-one (400 MHz, $CDCl_3$): δ=4.95~4.92 (1H, CH), 4.54~4.50 (1H, CH_2), 4.33~4.32 (1H, CH_2), and 3.77~3.64 ppm (2H, CH_2). * represents the residual solvent ethyl acetate. Reaction conditions: 60 ^{o}C, 48 h, yield of 99%.

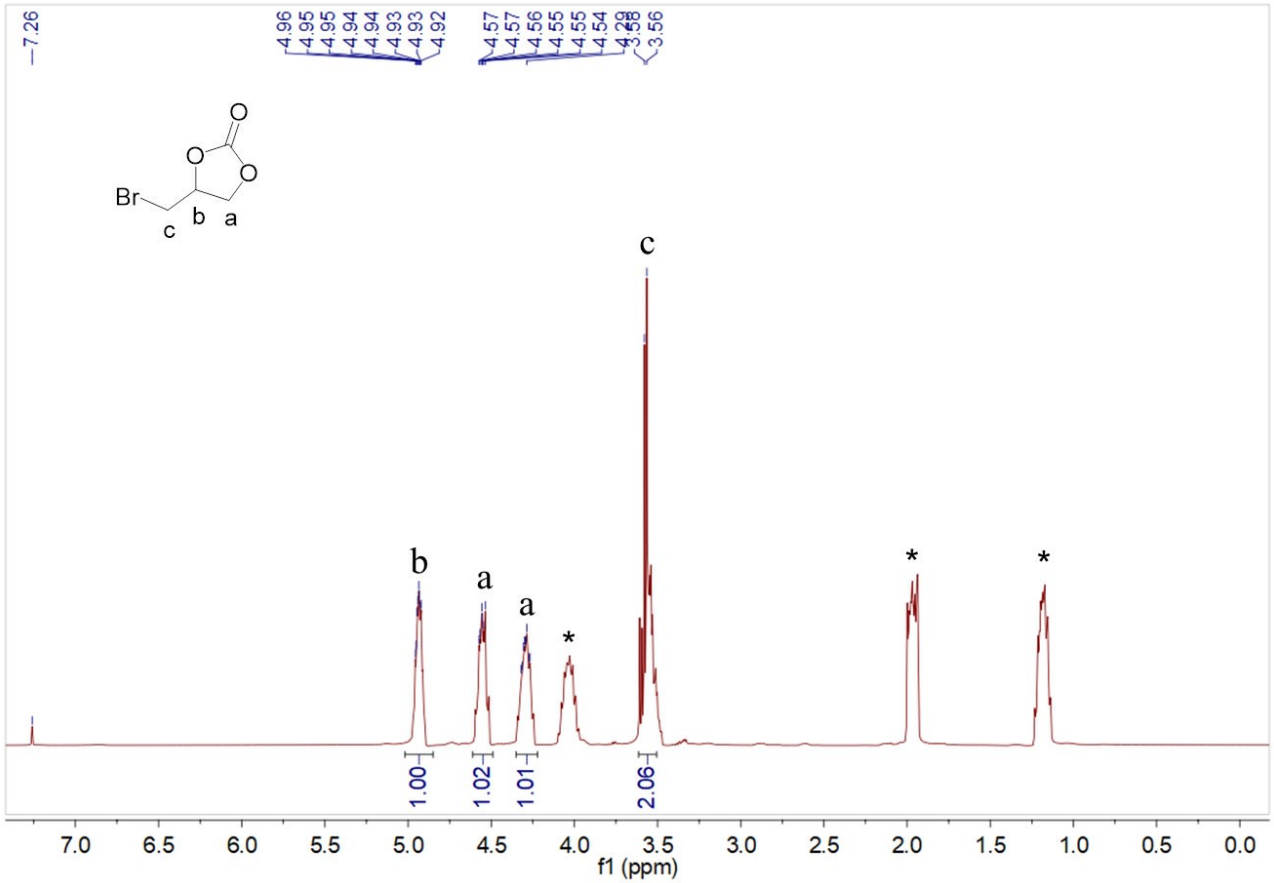

Fig. S13 ^{1}H NMR spectrum of 4-(bromomethyl)-1,3-dioxolan-2-one (400 MHz, $CDCl_3$): δ=4.96~4.92 (1H, CH), 4.57~4.54 (1H, CH_2), 4.29 (1H, CH_2), and 3.58~3.56 ppm (2H, CH_2). * represents the residual solvent ethyl acetate. Reaction conditions: 60 ^{o}C, 48 h, yield of 99%.

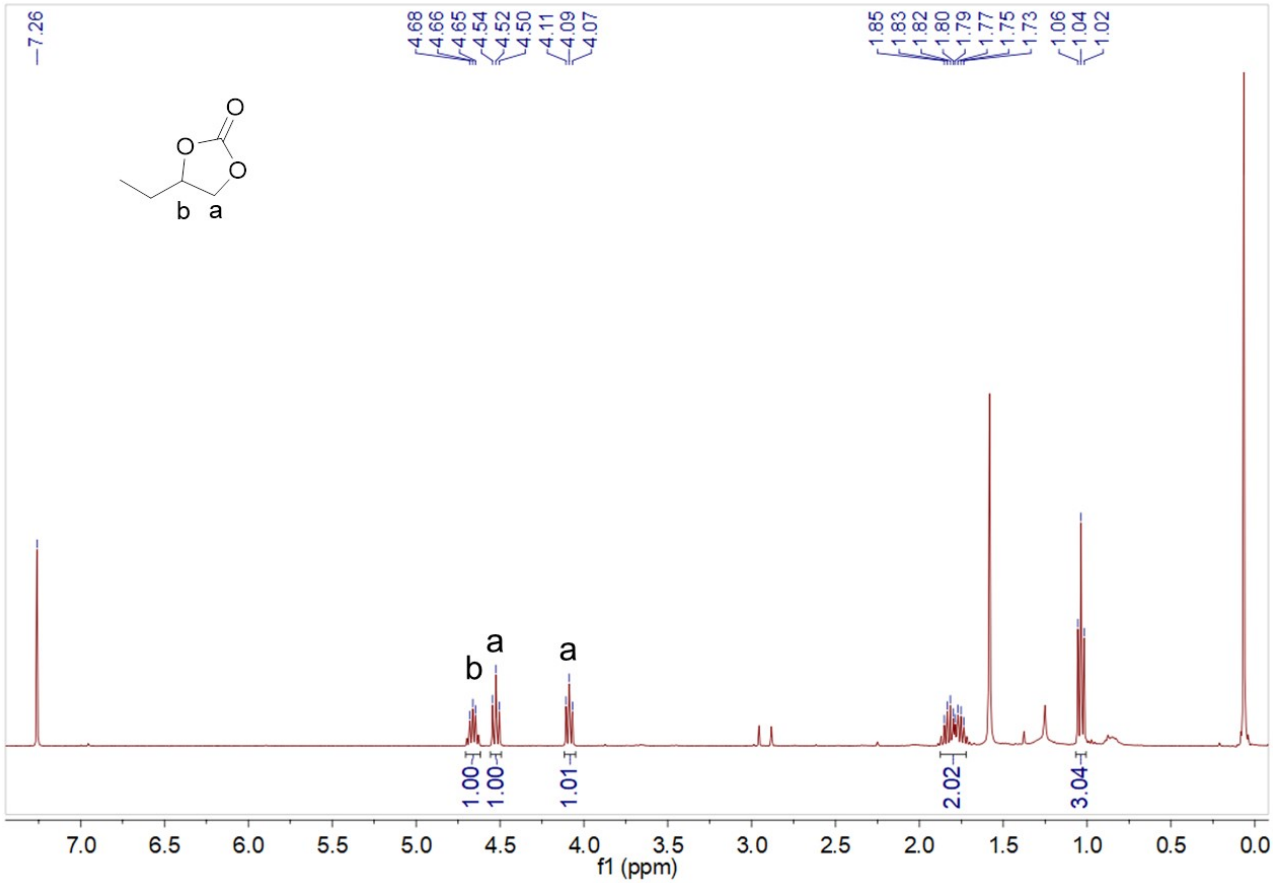

Fig. S14 ^{1}H NMR spectrum of 4-ethyl-1,3-dioxolan-2-one (400 MHz, $CDCl_3$): δ=4.68~4.65 (1H, CH_2), 4.54~4.50 (1H, CH_2), 4.11~4.07 (1H, CH_2), 1.85~1.73 (2H, CH_2), and 1.06~1.02 ppm (3H, CH_3). Reaction conditions: 40 °C, 72 h, yield of 99%.

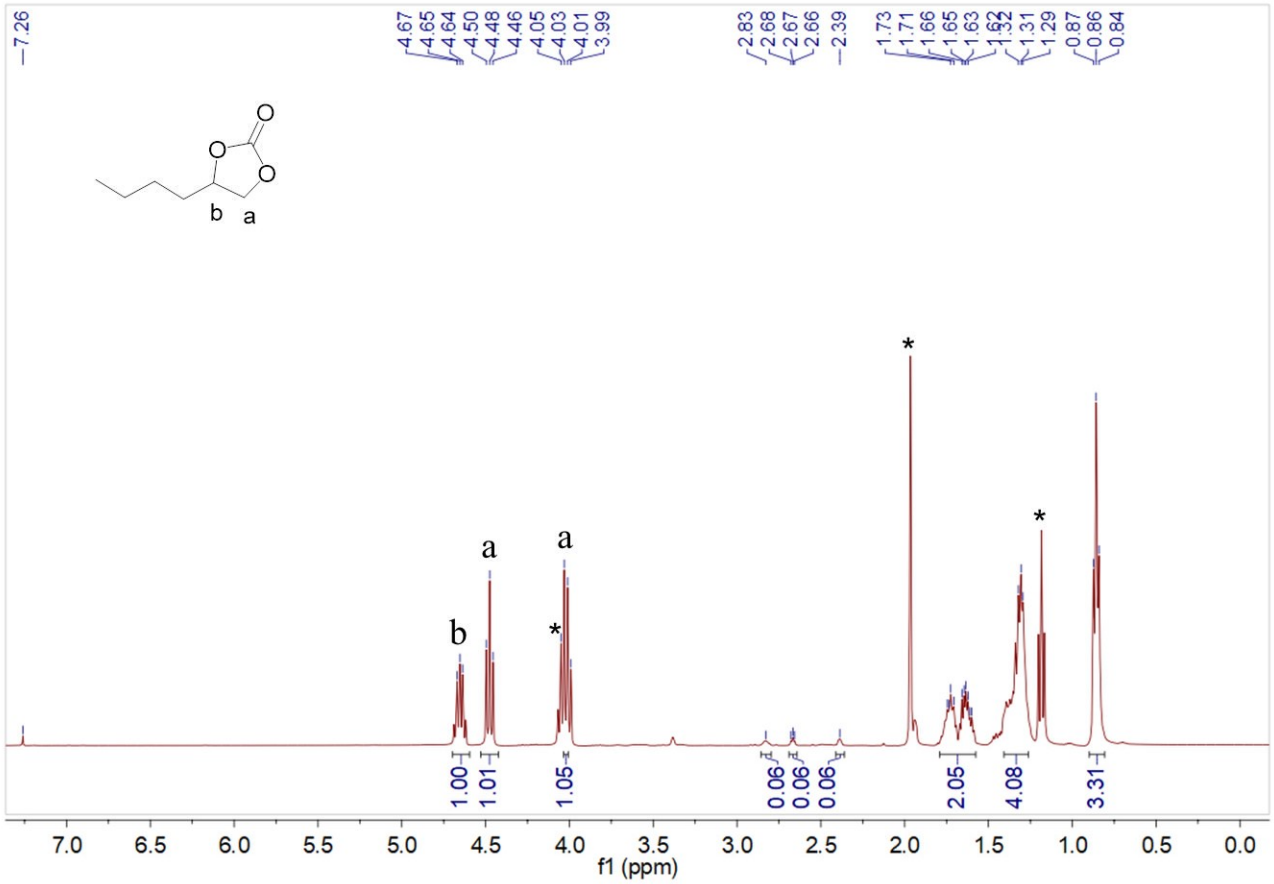

Fig. S15 ^{1}H NMR spectrum of 4-butyl-1,3-dioxolan-2-one (400 MHz, $CDCl_3$): δ=4.67~4.64 (1H, CH_2), 4.50~4.46 (1H, CH_2), 4.05~3.99 (1H, CH_2), 1.73~1.62 (2H, CH_2), 1.32~1.29 (4H, CH_2), and 0.87~0.84 ppm (3H, CH_3). * represents the residual solvent ethyl acetate. Reaction conditions: 80 ^{o}C, 72 h, yield of 94%.

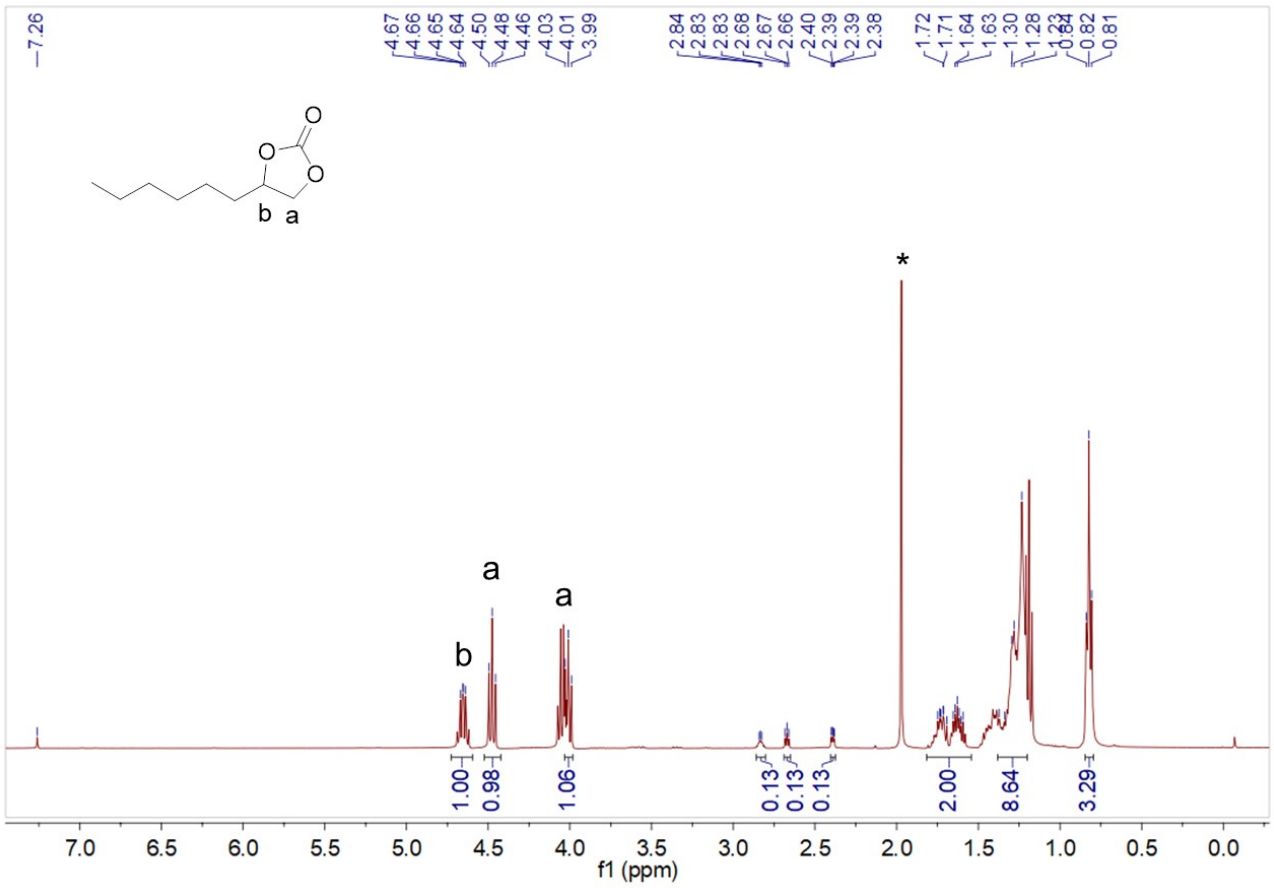

Fig. S16 ^{1}H NMR spectrum of 4-hexyl-1,3-dioxolan-2-one (400 MHz, $CDCl_3$): δ=4.67~4.64 (1H ,CH_2), 4.50~4.46 (1H, CH_2), 4.03~3.99 (1H, CH_2), 1.72~1.63 (2H, CH_2), 1.30~1.23 (8H, CH_2), and 0.84~0.81 ppm (3H, CH_3). * represents the residual solvent ethyl acetate. Reaction conditions: 100 ^{o}C, 72 h, yield of 88%.

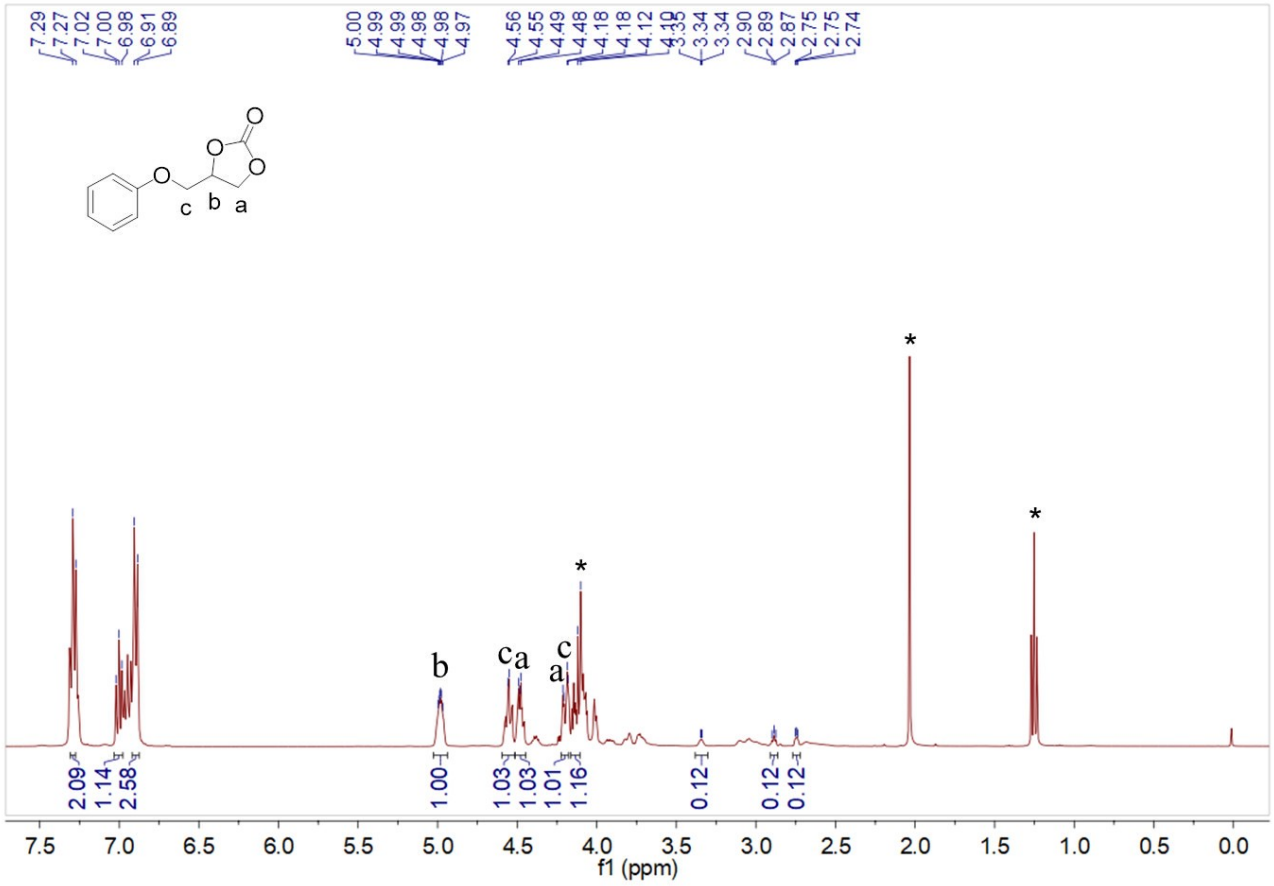

Fig. S17 ^{1}H NMR spectrum of 4-(phenoxymethyl)-1,3-dioxolan-2-one (400 MHz, $CDCl_3$): δ=7.29~7.27 (2H, CH), 7.02~6.98 (1H, CH), 6.91~6.89 (2H , CH), 5.00~4.97 (1H, CH), 4.56~4.55 (1H, CH_2), 4.49~4.48 (1H , CH_2), 4.18 (1H , CH_2), and 4.12~4.10 ppm (1H , CH_2). * represents the residual solvent ethyl acetate. Reaction conditions: 100 ^{o}C, 72 h, yield of 89%.

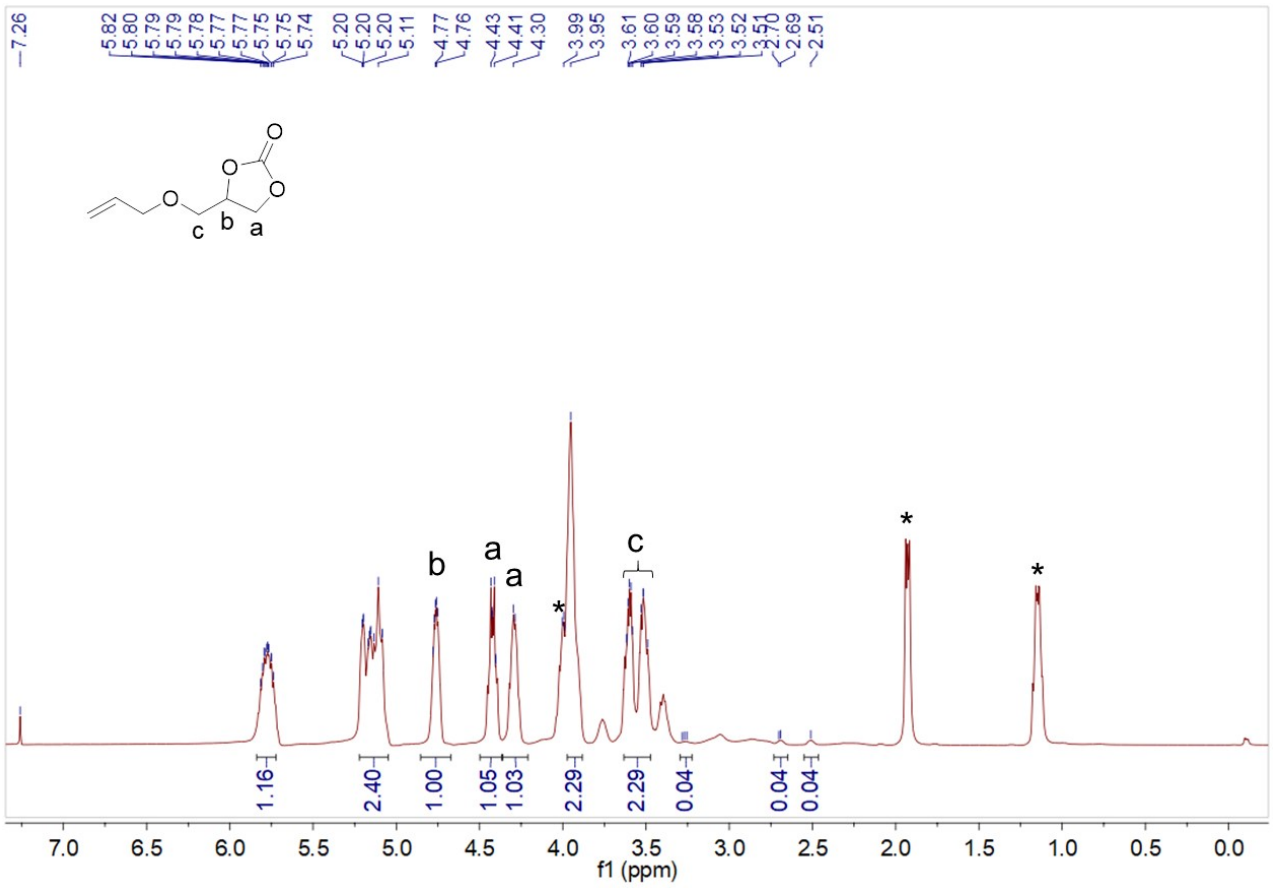

Fig. S18 ^{1}H NMR spectrum of allyloxymethyl-1,3-dioxolan-2-one (400 MHz, $CDCl_3$): δ=5.82~5.74 (1H, CH), 5.20~5.11 (2H, CH_2), 4.77~4.76 (1H, CH), 4.43~4.41 (1H, CH_2), 4.30 (1H, CH_2), 3.99~3.95 (2H, CH_2), and 3.61~3.51 ppm (2H, CH_2). * represents the residual solvent ethyl acetate. Reaction conditions: 120 ^{o}C, 72 h, yield of 96%.

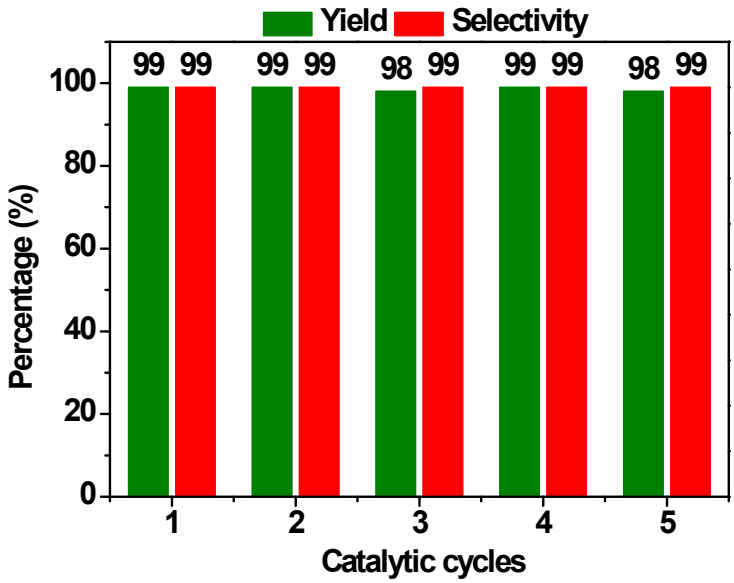

Fig. S19 A five-cycle assessment in the catalytic reusability of Py-iPOP-1 for the CO_2 conversion with glycidol. Reaction conditions: glycidol (2 mmol), CO_2 pressure (0.1 MPa), the catalyst (40 mg), 60 °C, 48 h.

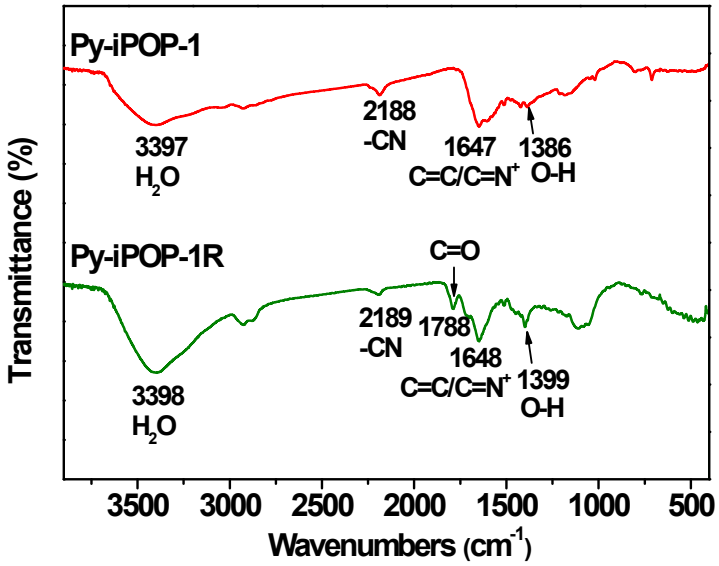

Fig. S20 FTIR of the fresh catalyst Py-iPOP-1 and the reused catalyst Py-iPOP-1R.

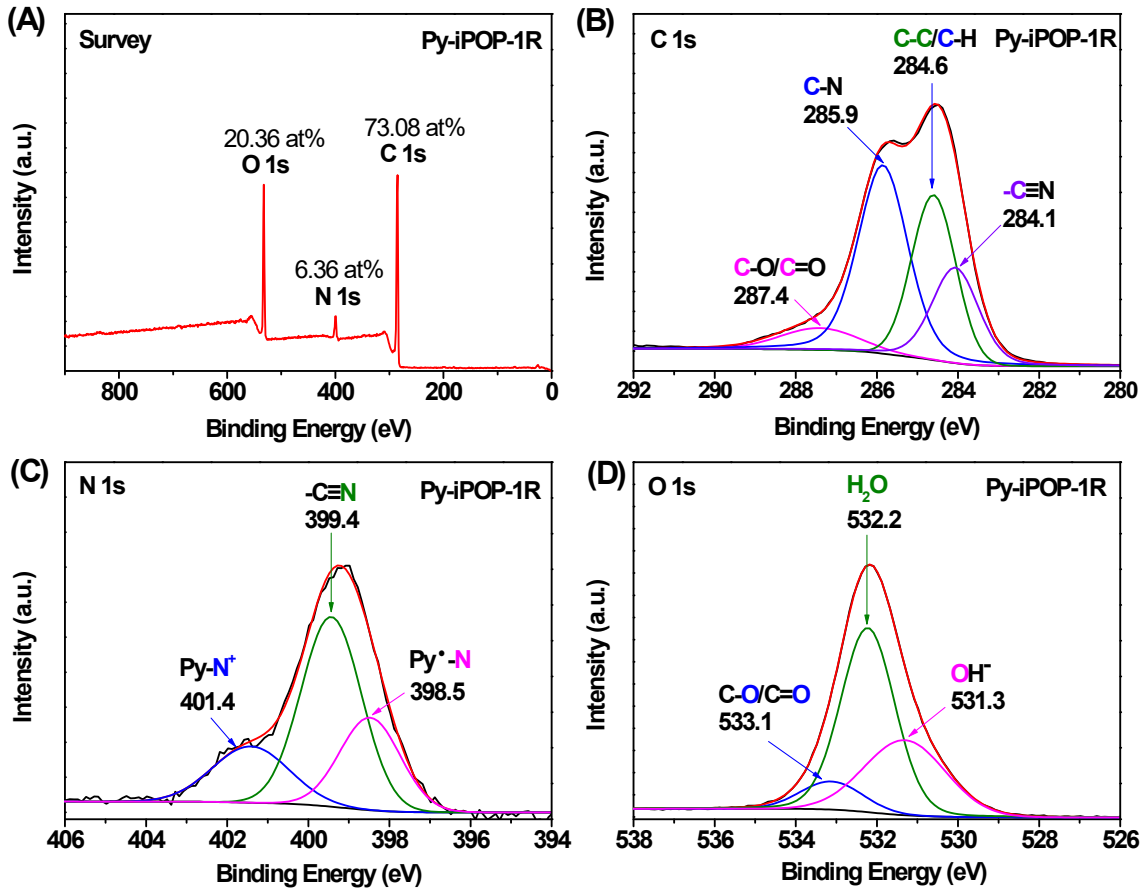

Fig. S21 XPS spectra of the reused catalyst Py-iPOP-1R: (A) Survey, (B) C 1s, (C) N 1s and (D) O 1s.

As shown in Fig. S20, FTIR spectrum of the reused catalyst Py-iPOP-1R shows a similar structure over the fresh one Py-iPOP-1. The newly appeared peak at 1788 cm^{-1} is assigned to the C=O stretching vibration originated from the absorbed product cyclic carbonate. As shown in Fig. S20A, compared with the fresh catalyst Py-iPOP-1 (Fig. S8), the relatively increased O content and decreased C and N contents in the XPS survey spectrum (Fig. S21A) indicates the existence of the absorbed product glycerol carbonate in the reused catalyst Py-iPOP-1R, which are also displayed by the newly appeared peaks at 287.4 eV (C-O/C=O) in the C 1s spectrum (Fig. S21B) and 533.1 eV (C-O/C=O) in the O 1s spectrum (Fig. S21D). The chemical structures and catalytic active sites including OH^- anions and pyridinyl radicals (Fig. S21C) were well retained, affording the good reusability of the heterogeneous catalyst Py-iPOP-1.

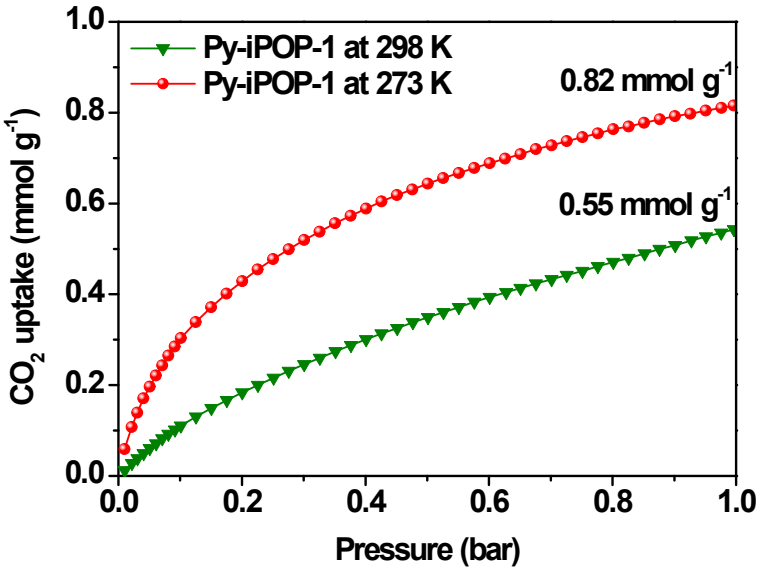

Fig. S22 CO_2 adsorption isotherms of Py-iPOP-1 collected up to 1.0 bar at 273 K and 298 K.

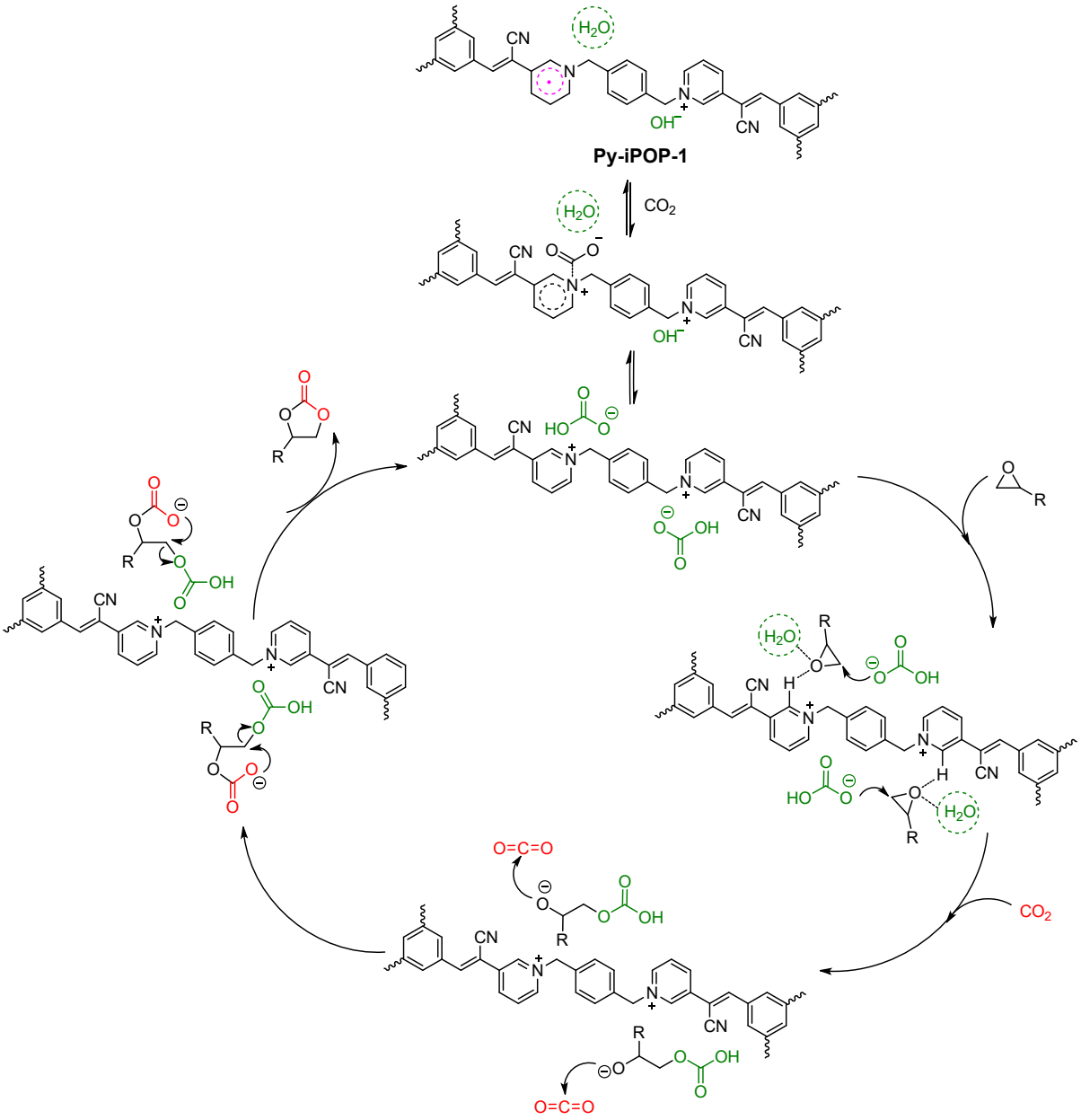

Scheme S4 A plausible catalytic mechanism for metal-free and halogen-free cycloaddition of epoxides with CO_2 over the catalyst Py-iPOP-1 with hydroxide anions and pyridinyl radicals.

References

(S1) S. Verma, G. Kumar, A. Ansari, R. I. Kureshy and N. H. Khana, *Sustainable Energy Fuels*, 2017, **1**, 1620–1629.

(S2) N. Zhang, B. Zou, G.-P. Yang, B. Yu, C.-W. Hu, *J. CO_2 Util.*, 2017, **22**, 9–14.

(S3) K. Thiel, R. Zehbe, J. Roeser, P. Strauch, S. Enthalerd and A. Thomas, *Polym. Chem*., 2013, **4**, 1848–1856.

(S4) Y.-M. Li, L. Yang, L. Sun, L. Ma, W.-Q. Deng and Z. Li, *J. Mater. Chem. A*, 2019, **7**, 26071–26076.

(S5) S. N.Talapaneni, O. Buyukcakir, S. H. Je, S. Srinivasan, Y. Seo, K. Polychronopoulou and A. Coskun, *Chem. Mater*., 2015, **27**, 6818–6826.

(S6) S. Subramanian, J. Park, J. Byun, Y. Jung and C. T. Yavuz, *ACS Appl. Mater. Interfaces*, 2018, **10**, 9478–9484.

(S7) Z. Guo, X. Cai, J. Xie, X. Wang, Y. Zhou and J. Wang, *ACS Appl. Mater. Interfaces*, 2016, **8**, 12812–12821.

(S8) Y. Zhou, W. Zhang, L. Ma, Y. Zhou and J. Wang, *ACS Sustainable Chem. Eng.*, 2019, **7**, 9387–9398.

(S9) X. Wang, Q. Dong, Z. Xu, Y. Wu, D. Gao, Y. Xu, C. Ye, Y. Wen, A. Liu, Z. Long and G. Chen, *Chem. Eng. J*., 2021, **403**, 126460.